Journal of Scientific Research & Reports

15(2): 1-13, 2017; Article no.JSRR.34929
ISSN: 2320-0227

Electrochemical, Spectrochemical and Quantum Chemical Studies on Dimedone as Corrosion Inhibitor for Copper in Acetonitrile

Pipat Chooto[1*] and Sontaya Manaboot[1]

[1]Analytical Chemistry Division, Department of Chemistry, Faculty of Science, Prince of Songkla University, Hatyai, Songkhla 90112, Thailand.

Authors' contributions

This work was carried out in collaboration between both authors. Author PC designed and analyzed the study as well as corrected the manuscript. Author SM conducted the experiments and outlined the manuscript. Both authors read and approved the final manuscript.

Article Information

DOI: 10.9734/JSRR/2017/34929
Editor(s):
(1) Mahmoud Nasr, Sanitary Engineering Department, Faculty of Engineering, Alexandria University, Egypt.
Reviewers:
(1) Mieczyslaw Scendo, Jan Kochanowski University in Kielce, Poland.
(2) Lebe Nnanna, Michael Okpara University of Agriculture, Nigeria.
(3) Prakasha Shetty, Manipal Institute of Technology, Manipal University, India.
Complete Peer review History: http://www.sciencedomain.org/review-history/20304

Original Research Article

Received 20th June 2017
Accepted 25th July 2017
Published 1st August 2017

ABSTRACT

The inhibition ability of 5,5-Dimethyl-1,3-cyclohexanedione (dimedone, DMD) for copper in acetonitrile at 25°C was investigated by potentiodynamic polarization and electrochemical impedance spectroscopy (EIS). Corrosion resistance increased with inhibitor concentration up to 93.68% inhibition efficiency at 3.00 mM, indicating that DMD molecules can cumulatively adsorb on the copper surface and finally form a protective film on copper-solution interface. This is also supported by the decreasing of copper oxidation in cyclic voltammogram. Polarization curves revealed that DMD is of mixed type inhibitor. The adsorption of DMD on copper surface obeys the Langmuir isotherm and the adsorption mechanism is of physisorption type. The standard energy of adsorption (ΔG^{o}_{ads}) values was found in good agreement for both polarization and impedance to be -8.17 and -8.43 kJmol^{-1} respectively. Fourier Transform Infrared spectroscopy (FT-IR) confirmed the interaction of copper with oxygen on DMD. The mole ratio method suggested that the complexation ratio of copper-DMD is 1:2. Scanning electron microscopy (SEM) of copper surface after immersion in DMD solution indicates the presence of a protective layer on the electrode surface. The frontier molecular orbital energy E_{HOMO} (highest occupied molecular orbital), E_{LUMO}

**Corresponding author: E-mail: pipat.c@psu.ac.th;*

(lowest unoccupied molecular orbital) and the Mulliken charge distribution obtained from Quantum chemical calculations revealed (ΔE) for DMD 0.2091 hartree, reflecting strong adsorption of the molecules on copper surface. The enhanced corrosion inhibition is possibly due to the compact film structure blocking electron transfer at the electrode surface.

Keywords: Copper; corrosion inhibition; organic inhibitor; electrochemistry.

1. INTRODUCTION

Copper metal is widely used in a number of fields as a structural component especially in marine systems [1-3] due to its desirable physicochemical, aesthetic and mechanical properties However, the presence of Cl^- makes it vulnerable to corrosion and makes corrosion inhibition economically important [3] due to the lost of partial or total replacement of equipment as well as structures and plant-repairing shutdowns.

The use of corrosion inhibitors is one of the most economical ways to reduce the corrosion rate, protect metal surfaces against corrosion and preserve industrial facilities [4]. Inorganic inhibitor is one of the simplest ways to improve the passivity of a metal by adding electropositive metal salts to the medium [5-7]. The inhibition is due to the reduction of electropositive ions followed by adsorption on the metal surface, which makes the metal more noble. However, recently increasing concern toward environmental and health consideration is likely to restrict inhibitor choices. A number of effective inhibitors such as chromate, phosphate, molybdate and nitrites will eventually be abandoned due to their toxicity [8]. Thus, there is still a need for testing and developing corrosion inhibitors that are effective and environmentally friendly in particular organic substitutes.

A number of organic compounds were found to have inhibitive properties including carboxylic acids, urea derivatives, amines, and other nitrogen containing compounds which can strongly adsorb onto the metal surface or react with the corrosion product on the surface to form a protective layer and provide a barrier to the dissolution of the metal in the electrolyte [9-14]. The efficiency of these organic corrosion inhibitors is related to the presence of polar functional groups including sulphur, nitrogen, oxygen and phosphorous atoms in their molecules as well as pi electrons especially in heterocyclic ring [15]. These polar groups are usually regarded as a reaction center for adsorption process. Consequently, in the light of corrosion inhibition, quinones with unpaired electrons of oxygen pi-bonds and conjugated benzene rings are possible to facilitate protective inhibition. Only a few experimental data on the inhibition properties of simple and substituted quinones are available in the literature [16].

The goal of the present study is to present the remarkable inhibiting properties of dimedone (DMD, Fig. 1), with greater advantages of cost effectiveness and non-toxicity. Due to the fact that DMD as well as involving complexes are slightly soluble in water and there are quite a few corrosion studies in nonaqueous conditions with less effect from oxygen and proton, here EIS and potentio-dynamic polarization were employed to evaluate corrosion rate of freshly polished copper and inhibition efficiencies of DMD as an inhibitor in acetonitrile. The copper surface was examined by SEM whereas the complexation between copper and DMD compounds was studied by CV, UV-Vis and FT-IR. The adsorption isotherm of DMD on copper surface and Quantum chemical parameters are also investigated to obtain more information about the mechanism of adsorption and corrosion inhibition of DMD on copper in acetonitrile.

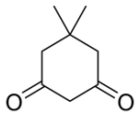

Fig. 1. Chemical structure of 5,5-Dimethyl-1,3-cyclohexanedione (DMD)

2. MATERIALS AND METHODS

2.1 Instruments

The electrochemical measurements were carried out by Methrom AUTOLAB PGSTAT 100 with GPES software as well as by Methrom AUTOLAB PGSTAT 302N with NOVA software. Quantum chemical calculations were performed with the use of Gaussian 09 package. The molecular structures of DMD was fully geometrically optimized using the functional RB3LYP DFT formation with electron basis 6-31G (d, p) for all atoms.

The Fourier Transform Infrared (FT- IR) spectrum was recorded with Perkin-Elmer FT-IR 783 model in KBr matrix at room temperature. The UV-Vis measurements were carried out by PerkinElmer Lambda 45 model and the surface morphology was analyzed by SEM of Quanta.

2.2 Electrochemical Cell Set-up

All electrochemical techniques were carried out using a standard three-cell electrode system consisting of a high purity platinum wire as a counter electrode (CE), silver-silver chloride (Ag/AgCl) as a reference electrode (RE) and a working electrode (WE) which was 99.98% copper coupons for potentiodynamic polarization and EIS techniques whereas a glassy carbon electrode (GCE, 2 millimeter diameter) for CV technique. The reference electrode was serviced regularly by changing the internal filling solution with a saturated solution of super-purum KCl (99.999+%).

2.3 Electrode Preparation

2.3.1 Electrochemical measurements

For potentiodynamic polarization and EIS, Cu was mechanically polished with emery paper (#1000), degreased with acetone, dried at room temperature and then immersed immediately in the test solution. No attempt was made to remove the air-formed oxide film which may have formed on the metal surface prior to immersion. In the case of CV GCE was polished with alumina (0.05 μm) water slurry on polishing cloth, rinsed well with distilled water and wiped several times with wetted soft tissue.

2.4 Sample Preparation

2.4.1 Electrochemical measurement

For potentiodynamic polarization and EIS, appropriate amount of DMD was dissolved and the volume made up with acetonitrile. In the case of supporting electrolyte for CV, 0.3880 g of $TBAPF_6$ was dissolved with acetonitrile and the volume was made up to 100 mL. 1.0×10^{-3} M $CuCl_2{\cdot}2H_2O$ was prepared by dissolving 0.0170 g of $CuCl_2{\cdot}2H_2O$ and its volume was made up to 100 mL with 0.0100 M $TBAPF_6$ in acetonitrile. DMD 0.0140 g was dissolved and diluted to 100 mL to obtain 1.0×10^{-3} M solution. The mixture of Cu (II) and DMD solution was prepared by adding 0.0085 g of $CuCl_2{\cdot}2H_2O$ in 50 mL 1.0×10^{-3} M DMD with 0.010 M TBAF in acetonitrile.

2.4.2 Spectroscopic measurement

For UV-Vis spectroscopy, 1.0×10^{-3} M $CuCl_2{\cdot}2H_2O$ was prepared by weighing 0.0170 g of $CuCl_2{\cdot}2H_2O$ and dissolved in acetonitrile and the volume was made up to 100 mL. DMD 0.0140 g was prepared in the same way to obtain the concentration of 1.0×10^{-3} M.

For FTIR, copper-DMD complex solution was prepared by weighing 0.2800 g of DMD (2.0×10^{-3} mol) and dissolved in 20.0 mL of methanol. $CuCl_2{\cdot}2H_2O$ 0.1705 g (1.0×10^{-3} mol) in 15 mL of methanol was added and the solution was refluxed at 70°C for 5 hours. After filtering, the filtrate was left at room temperature for 1 month to obtain green crystals. Which were further isolated by suction filtration, washed with acetone and dried in a vacuum desiccator. The sample obtained was ground to reduce the particle size to less than 5 mm in diameter. A small amount of powder sample (about 0.1-2% of the KBr amount, or just enough to cover the tip of spatula) was mixed with the KBr powder, subsequently ground for 3-5 min and then pressed to form a thin and transparent pellet.

2.5 Procedure

2.5.1 Electrochemical measurement

In polarization measurement, 50 mL of the test solution was pipetted into the 100 mL cell. The measurements were made after allowing the electrode to achieve the steady state potential under open-circuit condition at room temperature. The nature of inhibitor was interpreted via polarization curves with a scan rate of 0.5 mV/s on freshly-prepared copper electrodes. Inhibition efficiencies were then evaluated (*vide infra*) from corrosion current densities (j_{corr}) obtained by Tafel extrapolation method.

Impedance measurement was carried out in the same way as polarization measurement. Impedance spectra were obtained in the frequency range of 0.1 Hz to 150 kHz with perturbation amplitude of 10 mV. Inhibition efficiencies were evaluated from charge transfer resistance (R_{ct}).

CV studies were carried out in a glass cell with a capacity of 100 ml. 50 mL mixture of Cu (II) and DMD solution was pipetted into the cell and

cyclic voltammograms were recorded in the potential range of -1.8 to 1.8 V with scan rate of 100mV/s.

2.5.2 Spectroscopic measurements

2.5.2.1 UV-Vis spectroscopy

In the mole ratio method, different aliquots of DMD solution were added in 3.0 mL of 1.0 × 10^{-3} M copper (II) solution in order to get various metal ligand ratios ranging from 1:0.8 to 1:4.0. The absorbance was recorded at λmax 246 nm and temperature maintained at 25°C.

2.5.2.2 FTIR

The chemical structure of the sample was determined by using absorption FTIR spectroscopy at a resolution of 4 cm^{-1}. 16 additive scans were carried out between 4000 to 400 wave numbers.

2.5.3 Microscopy by SEM

After preparation, 1.0 × 1.0 cm^2 Cu electrodes were immersed in the test solution for 6 h, dried at room temperature and then investigated by SEM.

2.5.4 Quantum chemical calculations

Quantum chemical calculations using density functional theory (DFT) methods were applied to give values of the highest occupied molecular orbital (E_{HOMO}), lowest unoccupied molecular orbital (E_{LUMO}), dipole moment (D) and Mulliken atomic charge distribution of the DMD molecule, which are useful in explaining electron density in forming complex with metal.

3. RESULTS AND DISCUSSION

3.1 Cyclic Voltammetry and Mole Ratio

The preliminary information about how DMD can influence the corrosion process of copper is pointed by its electrochemical behavior. The redox behavior of Cu (II) in copper (II) chloride in 0.01 M $TBAPF_6$ in acetonitrile by cyclic voltammetry on glassy carbon electrode at 25°C confirms the formation of Cu (II) DMD complex (Fig. 2). The shift of both reduction peaks of Cu (II) to more negative reveals less electron density which makes accepting electron more difficult. On the other hands, oxidation peaks shift to more positive which also indicates less possibilities in transferring electron due to complex formation. Similar behaviors are found for the case of peaks from DMD, especially oxidation. The complexation ratio of copper-DMD was also found to be 1:2 by mole ratio method.

3.2 Potentiodynamic Polarization

Fig. 3 illustrates the potentiodynamic polarization curves of copper in acetonitrile with and without DMD from which relevant parameters are obtained (Table 1) namely corrosion potential (E_{corr}), anodic and cathodic Tafel slopes (β_a, β_c), polarization resistance (R_p), corrosion current density (j_{corr}), corrosion rate (ν_{corr}), surface coverage degree (θ) and corrosion inhibition efficiency (IE%).

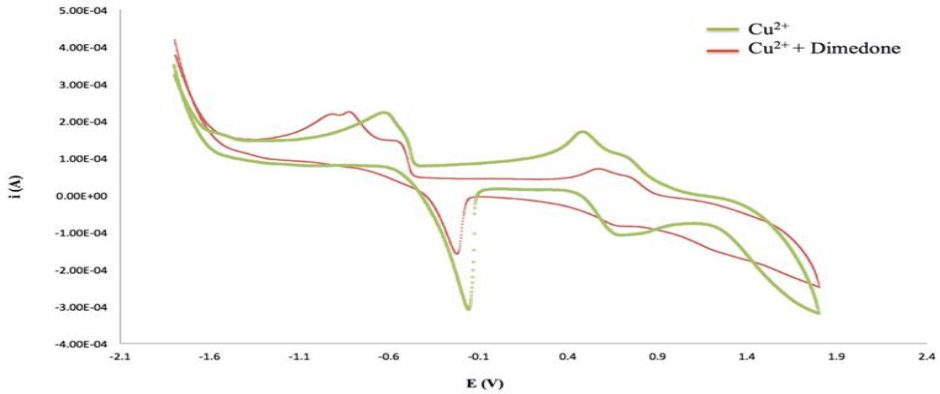

Fig. 2. Cyclic Voltammogram of 1.00 mM of $CuCl_2.2H_2O$ at -1.800 – 1.800 V potential window and 100 mVs^{-1} scan rate in the presence of 0.01 M $TBAPF_6$ as supporting electrolyte in acetonitrile at 25°C

The presence of DMD causes small fluctuations of E_{corr} between -0.24 V and -0.30 V and the change of β_a and $-\beta_c$, indicating that DMD acts as a mixed-type corrosion inhibitor which suppresses both anodic and cathodic reaction simultaneously [17]. This suppression of the corrosion process possibly results from adsorbed DMD molecules on copper surface which blocks corrosion mechanism. Furthermore, by increasing DMD concentration, j_{corr}, ν_{corr} greatly decrease and the IE% calculated from j_{corr} (Eq. (3)) increases. Also, θ increases with DMD concentration. At low DMD concentrations in solution, it can be concluded that they obstruct the corrosion by merely preventing the reaction sites on copper surface.

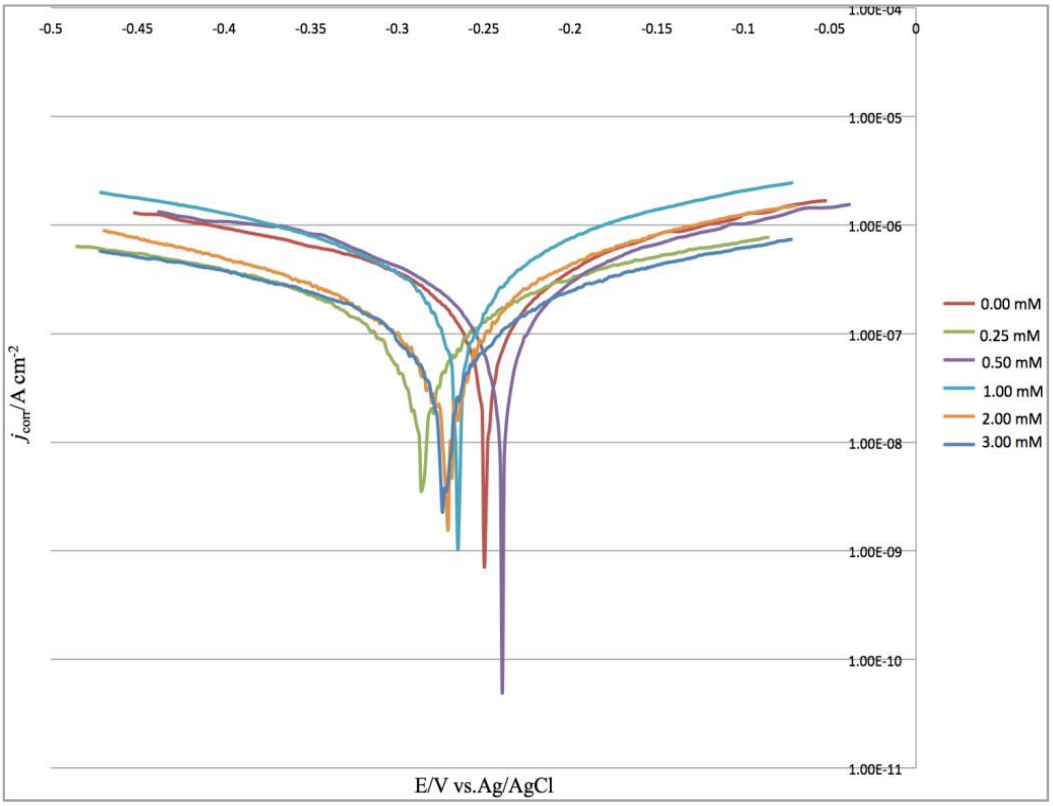

Fig. 3. Potentiodynamic polarization curves for copper in acetonitrile with DMD at various concentrations at 25°C and 0.5 mVs^{-1} scan rate

Table 1. Polarization parameters of copper in acetonitrile solution in absence and presence of DMD at different concentrations at 25°C

C_{inh} (mM)	E_{corr} (V vs Ag/ AgCl)	β_a (V dec^{-1})	$-\beta_c$ (V dec^{-1})	R_p (mΩ)	j_{corr} (μA cm^{-2})	ν_{corr} (μm year^{-1})	θ	IE%*
0.00	-0.26	31.56	1.28	140.66	3.81	44.20	-	-
0.25	-0.29	7.13	2.66	281.14	2.47	28.70	0.35	35.17
0.50	-0.24	1.84	1.34	138.24	2.44	28.30	0.36	35.95
1.00	-0.27	0.90	0.56	96.17	1.56	18.10	0.59	59.06
2.00	-0.27	0.76	0.36	205.43	0.52	6.00	0.86	86.48
3.00	-0.30	0.30	0.22	122.94	0.44	5.10	0.88	88.37

The j_{corr} of copper was determined using the relation (1) and the ν_{corr} and IE% with equations (2) and (3):

$$i_{corr} = \frac{\beta_a \beta_c}{2.303 \times R_p \times (\beta_a + \beta_c)} \quad (1)$$

where 2.303 is the conversion factor

$$\nu_{corr} = \mu_{eq} K_p \frac{j_{corr}}{\rho} \quad (2)$$

where μ_{eq} is equivalent weight of copper (31.78 amu), K_p is a proportionality constant (3.27×10^{-3}) and ρ is copper density (8.96 g/cm^3)

$$IE\% = \frac{j_{corr}(uninh) - j_{corr}(inh)}{j_{corr}(uninh)} \times 100 \quad (3)$$

where j_{corr}(inh) and j_{corr}(uninh) are the corrosion current densities for copper electrode in acetonitrile with and without DMD respectively.

3.3 EIS Measurement

The influence of DMD on the adsorption process and corrosion inhibition on copper surface can be partially obtained by EIS. The Nyquist diagram for copper in acetonitrile solution, without and in the presence of different concentrations of DMD, were similar in shape (Fig. 4) of a single semicircle which indicates the corrosion reaction is controlled by the charge transfer process [18-20].

Typical Bode EIS plots obtained for copper in acetonitrile, without and in the presence of different concentrations of DMD are shown in Fig. 5. It can be seen that the impedance values of the copper are lower at high frequency, increases with decreasing frequency, and slightly increased at the lowest frequency. By increasing DMD concentration, the impedance of copper at low frequencies attained higher values. This demonstrates that the copper surface is more passivated due to the adsorption of DMD molecules on the Cu surface [21].

With the analysis of impedance data using the equivalent circuit (EC) as shown in Fig. 6, charge transfer resistance (R_{ct}) and double-layer capacitance (C_{dl}) were obtained (Table 2).

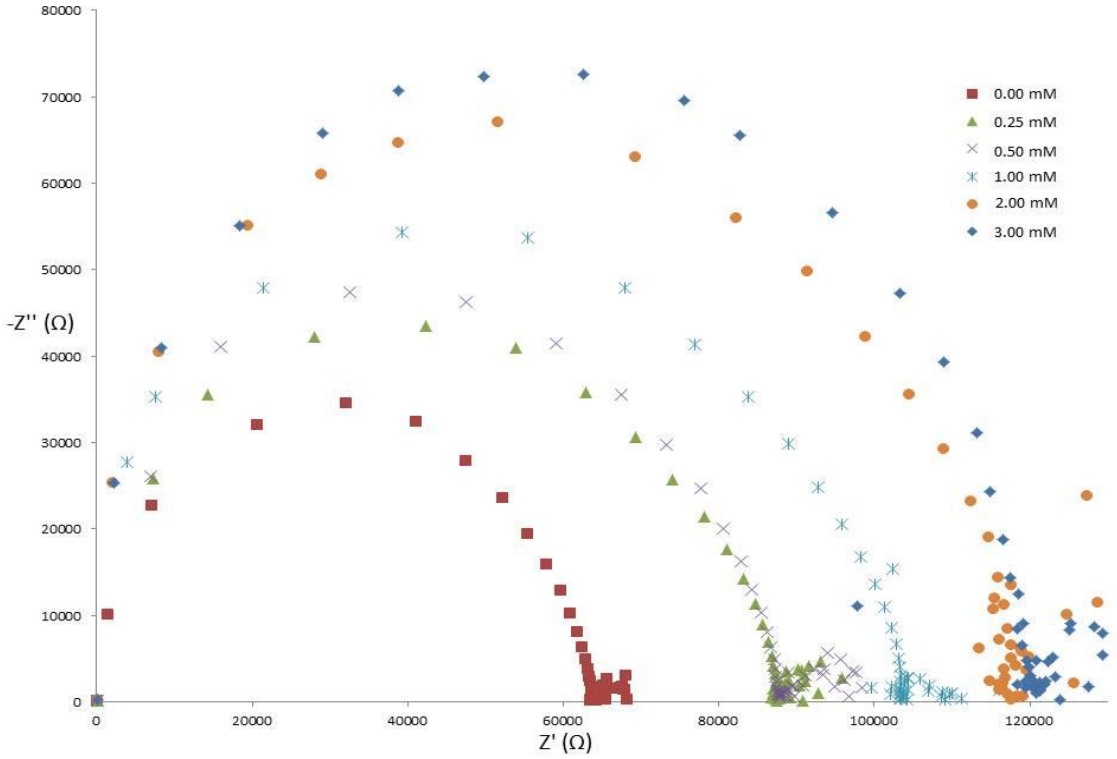

Fig. 4. Nyquist plots copper in acetonitrile solution containing various concentrations of DMD at 25°C

Table 2. Electrochemical impedance parameters for copper in acetonitrile solution in the absence and presence of DMD at different concentrations at 25°C

C_{inh}/mM	R_s/Ω cm^2	R_{ct}/kΩ cm^2	C_{dl}/pF	θ	IE%*
0.00	257.60	63.71	72.40	-	-
0.25	262.10	88.18	41.50	0.38	38.41
0.50	245.62	88.74	38.00	0.39	39.29
1.00	258.00	104.54	28.00	0.64	64.09
2.00	250.32	117.84	20.00	0.84	84.95
3.00	261.49	123.40	17.80	0.94	93.68

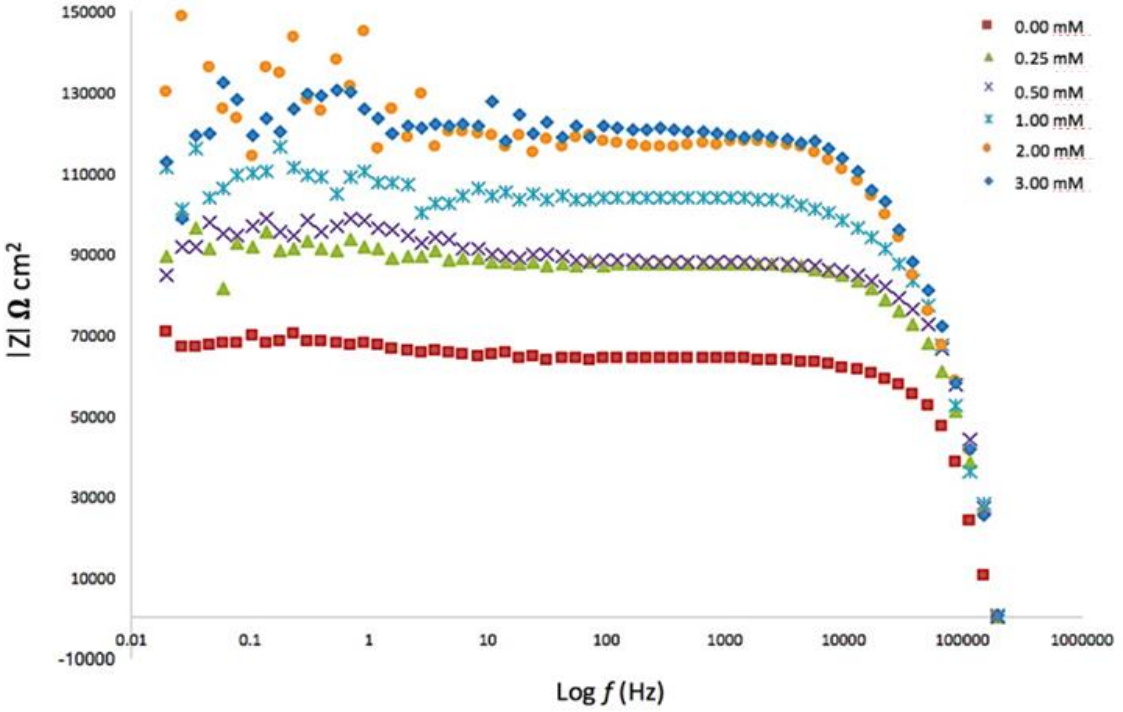

Fig. 5. Bode plots copper in acetonitrile solution containing various concentrations of DMD at 25°C

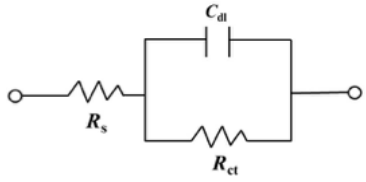

Fig. 6. Equivalent circuit (EC) model used to fit the experimental impedance data. In which R_s represent the solution resistance, R_{ct} charge transfer resistance C_{dl} are constant phase elements for double layer

It is apparent that the (R_{ct}) values of copper in acetonitrile solution significantly increased with increasing amount of DMD, indicating that the presence of DMD improved copper corrosion inhibition. Additionally, the decrease in C_{dl} values caused both the decrease in the dielectric constant and the increase of the double layer thickness, also supporting the adsorption of DMD on the copper/solution interface [21]. Finally, progressive covering of copper surface by DMD leads to the maximum inhibition efficiency of 93.68% with DMD at the 3.0 mM (Table 2), in good agreement with polarization results. With the concentration over 3.00 mM, %IE was only slightly increased which was possibly due to surface saturation. The R_{ct} and C_{dl} are calculated from Eq. (4):

$$f(-Z''\_\max) = \frac{1}{2\pi C_{dl} R_{ct}} \quad (4)$$

where ($-Z''_{max}$) is the maximum imaginary component of the impedance, and %IE is calculated from R_{ct} data by Eq. (5)

$$IE\% = \frac{R_{ct} - R^0_{ct}}{R^0_{ct}} \times 100 \quad (5)$$

where R_{ct} and R^0_{ct} are the charge transfer resistance with and without DMD, respectively.

3.4 Adsorption Isotherm

The adsorption isotherm is an effective way to explain the adsorption mechanism of the inhibitors [22]. A number of adsorption isotherms were tested for DMD adsorption on copper, including Freundlich, Temkin, Flory-Huggins and Langmuir. Langmuir isotherm was found to provide the best description for the adsorption behaviour of DMD as follows [11]:

$$\frac{C_{inh}}{\theta} = \frac{1}{K_{ads}} + C_{inh} \quad (6)$$

where C_{inh} is the inhibitor concentration, K_{ads} the equilibrium constant for adsorption process and θ the surface coverage degree by inhibitor molecules and the metal surface.

The surface coverage degree θ (Table 1 and Table 2) was calculated by IE%/100 [19] from both impedance and polarization measurements with good agreement of linear relationships between C/θ and C as shown in Fig. 7. Linear correlation coefficients (R^2) of 0.9652 and 0.9780 from potentiodynamic polarization and EIS techniques respectively, indicating that the adsorption of DMD on copper surface at 25°C obeys the Langmuir adsorption isotherm [11].

K_{ads} can then be calculated from the intercepts to be 1.38 and 1.54 mM from potentiodynamic polarization and EIS respectively. K_{ads} is related to standard energy of adsorption (ΔG^o_{ads}) by the equation [19]:

$$\Delta G^o_{ads} = -RTln(19.147K_{ads}) \quad (7)$$

where 19.147 is the concentration in M of acetonitrile. Calculated ΔG^o_{ads} from impedance and polarization data was -8.43 and -8.17 kJmol^{-1} respectively. G^o_{ads} of -20 kJmol^{-1} or lower indicates physisorption whereas that about -40 kJ mol^{-1} involves charge sharing or a transfer from the inhibitor molecules to the metal surface to form a coordinate type of bond (chemisorption) [23]. Hence the adsorption of DMD compounds is of physisorption type. The negative values of ΔG^o_{ads} reveal the spontaneity of adsorption process and stability of the adsorbed layer on the copper surface.

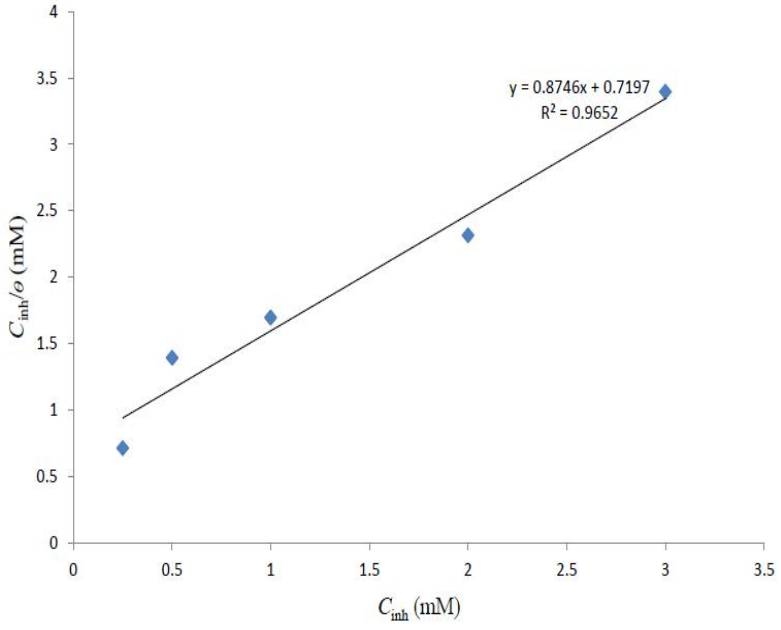

(a)

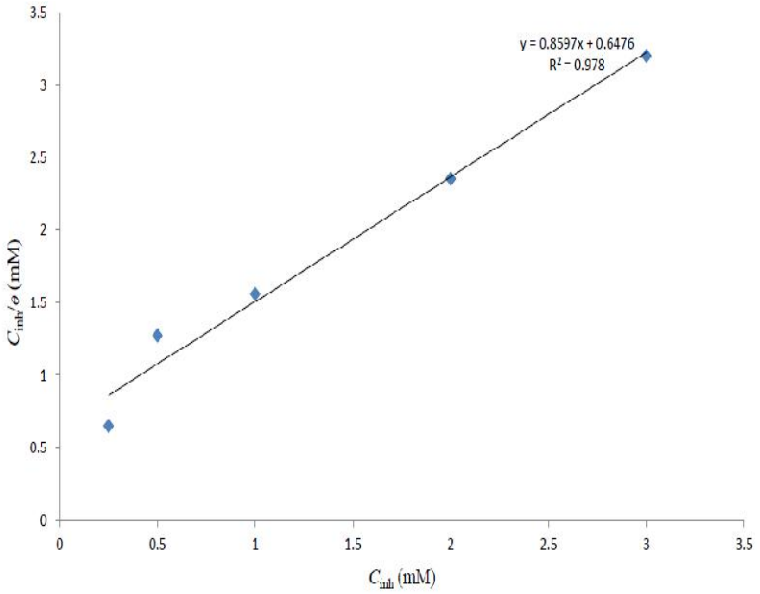

(b)

Fig. 7. Langmuir adsorption isotherm by impedance (a) and polarization (b) measurement of DMD on copper surface in acetonitrile at 25°C

3.5 Fourier Transform Infrared Spectroscopy (FT-IR)

Fig. 8 shows FT-IR spectrum of solid DMD on KBr pellet. The spectrum shows a peak bands of C-H stretching at 2956.09 cm^{-1}, C=O stretching at 1733.82 cm^{-1} and C-H bending at 1411.74 cm^{-1}. The same characteristic bands appeared for Cu (II) DMD complex with strong C=O stretching modification (Fig. 9 and Table 3): C=O stretching had disappeared due to the complex formation between C=O and Cu, C-H stretching at 2961.00 cm^{-1} and C-H bending at 1421.66 cm^{-1} [24]. The shift indicates the *change of* electron cloud density due to the coordination with Cu (II) [25].

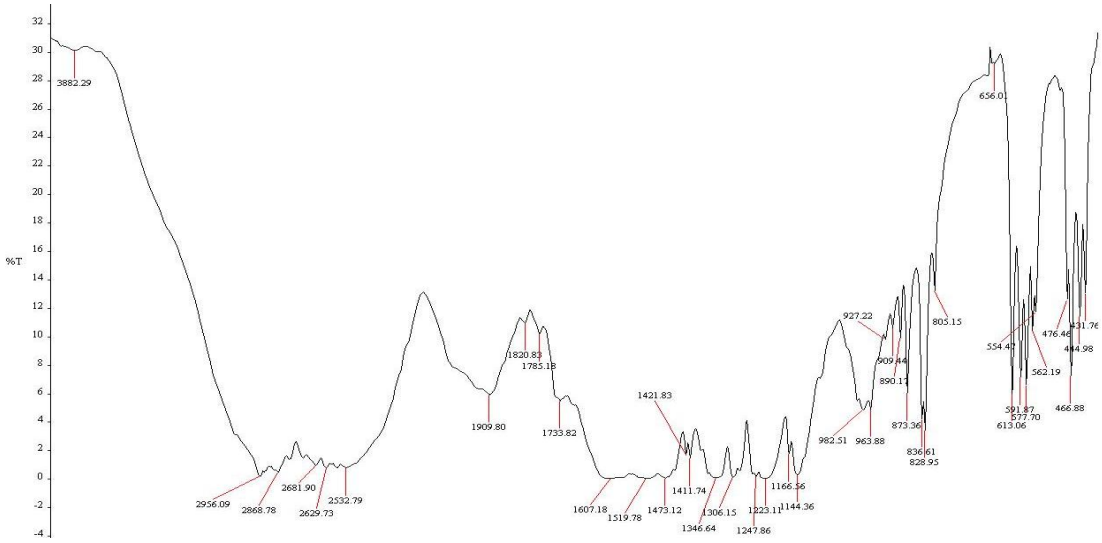

Fig. 8. IR spectrum of DMD

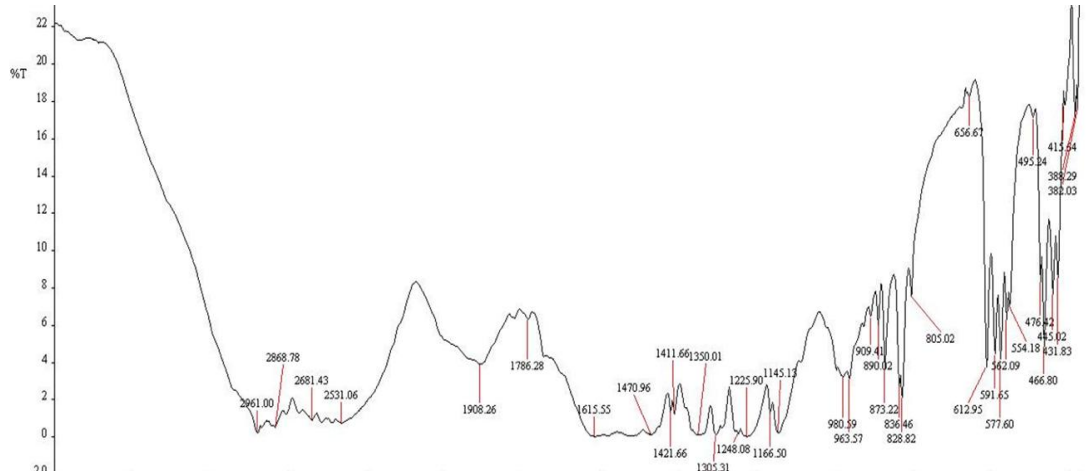

Fig. 9. IR spectrum of DMD and $CuCl_2 \cdot 2H_2O$

Table 3. Frequencies of the bands in the IR spectra of DMD and DMD-$CuCl_2$ complex

Functional group vibration	DMD	DMD with $CuCl_2 \cdot 2H_2O$
C-H stretching	2956.09 cm^{-1}	2961.00 cm^{-1}
C=O stretching	1733.82 cm^{-1}	disappear
C-H bending	1411.74 cm^{-1}	1421.66 cm^{-1}

3.6 Morphological Studies of Copper Surface

Copper surface was characterized by SEM whose results without DMD shown in Fig. 10 (a) indicate smooth surface with certain scratches on the bare copper surface caused by polishing in the electrode cleaning process. Similarly, copper surface after removing the layer of DMD (Fig. 10 (b)) shows the same characteristics as that in the case of the bare copper. With DMD, a protective layer is shown (Fig. 10 (c)) in good accordance with the results obtained from potentiodynamic measurements and EIS.

3.7 Quantum Chemical Calculations

To investigate the effect of molecular structure on inhibition mechanism, quantum chemical calculations were performed for neutral species. The geometry of DMD compound was determined by optimizing all geometrical variables without any symmetry constraints to obtain the result shown in Fig. 11(c). Certain quantum chemical parameters are related to the interactions between the inhibitor and the copper surface including E_{HOMO}, E_{LOMO} and dipole moment (D). E_{HOMO} is associated with the capacity of a molecule to donate electrons and the increase in the value of E_{HOMO} can facilitate adsorption hence the inhibition efficiency, which also indicates the disposition of the molecule to donate orbital electrons to an appropriate acceptor with empty molecular orbitals [26]. In contrast, E_{LUMO} indicates the ability of the molecule to accept electrons. The lower the value of E_{LUMO}, the more probable is the molecule to accept electrons. Low absolute value of the energy band gap (E_{HOMO} - E_{LUMO}) renders good inhibition efficiencies because it means lower energy to remove an electron from the highest occupied orbital [26].

DMD was found to have high HOMO (-0.2449 hartree (Table 4)) with the preferred active sites for an electronic attack and the favourite sites for interaction with the metal surface located at 1,3-cyclohehadione in the molecule (Fig. 11 (a)) whereas its E_{LUMO} is low (-0.03583 hartree). Additionally, low energy gap of 0.2091 hartree support DMD high inhibitory performance. The dipole moment of the molecule is also calculated due to the fact that it is influenced by the molecular structure and is expected to play a role in the adsorption process [26]. High D of DMD (3.6935, Table 4) reveals the favor of the molecule to accumulate on the surface layer and in turn reduce the rate of electrochemical reaction [27].

Table 4. Quantum chemical parameters of DMD

E_{HOMO} (hartree)	E_{LUMO} (hartree)	ΔE (hartree)	Dipole moment(D)
-0.2449	-0.0358	0.2091	3.6935

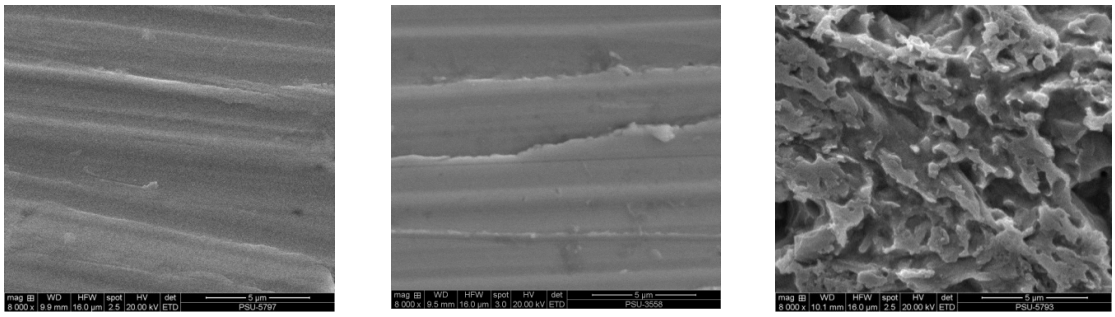

(a) (b) (c)

Fig. 10. SEM micrographs of (a) bare copper surface (b) copper surface after removing the layer of DMD and (c) copper surface in the presence of 3.00 mM DMD after 6 h

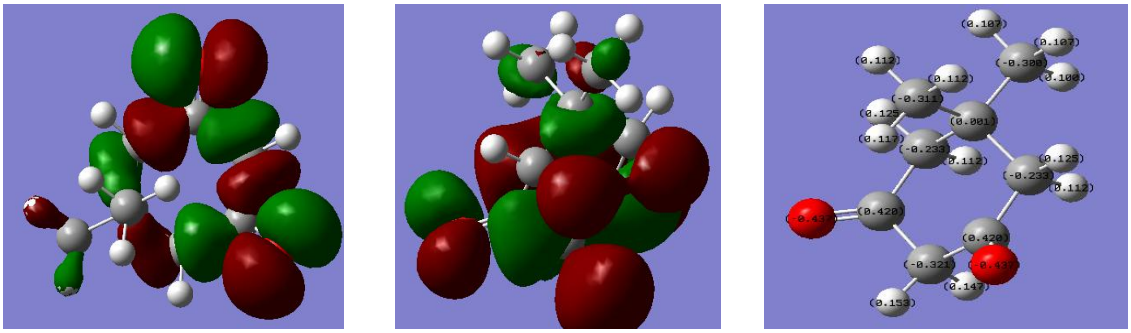

(a) (b) (c)

Fig. 11. (a) E_{HOMO}, (b) E_{LUMO}, and (c) Mulliken atomic charge distribution of DMD molecule calculated by RB3LYP DFT method

The Mulliken atomic charge distribution calculated using the DFT method is presented in Fig. 11 (c). Oxygen and some carbon atoms have higher charge densities so they are generally the sites where electrophiles attack. Therefore, O and C atoms were active centers with the ability to form a protective film by physical adsorption with copper surface. In addition, the HOMO (Fig. 11 (a)) was mainly distributed on 1,3-cyclohexanedione, the framework of DMD, which therefore probably the primary site in forming a protective film. It could be deduced on the above discussion that DMD, apart from existing in the anionic form which can interact with copper surface by electrostatic attraction, may also interact with the copper surface via oxygen and carbon atoms, forming an effective protective layer on the copper surface thus retarding further corrosion of the metal in acetonitrile.

4. CONCLUSION

Inhibition efficiency of DMD towards copper corrosion in acetonitrile solution was determined by electrochemical techniques including polarization and impedance measurements to obtain 88.37 and 93.68% respectively. Potentiodynamic polarization revealed that DMD is a mixed-type corrosion inhibitor with efficiency which increases with concentration. Protection afforded by DMD is due to its physical adsorption obeying Langmuir isotherm. The adsorption layers and corresponding complexes formed by DMD are further confirmed by the results from CV, SEM, UV-Vis and FTIR analysis. From

calculated standard energy of adsorption and quantum chemical calculations, the driving force for the formation of protective film could be the physisorption via the oxygen and carbon atoms.

COMPETING INTERESTS

Authors have declared that no competing interests exist.

REFERENCES

1. Liu X, Hu W, Yang S, Li Z, Pei C, Zhou Y, Yin G. Severe corrosion of copper in a highly alkaline egg white solution due to a biuret corrosion reaction. Corros. Sci. 2015;94:270–274.
2. Melchers ER. Bi-modal trends in the long-term corrosion of copper and high copper alloys. Corros. Sci. 2015;95:51–61.
3. Tian H, Li W, Cao K, Hou B. Potent inhibition of copper corrosion in neutral chloride media by novel non-toxic thiadiazole derivatives. Corros. Sci. 2013; 73:281-291.
4. Yıldırım A, Çetin M. Synthesis and evaluation of new long alkyl side chain acetamide, isoxazolidine and isoxazoline derivatives as corrosion inhibitors. Corros. Sci. 2008;50:155-165.
5. Antonijevic MM, Petrovic MB. Copper corrosion inhibitors. A review. Int. J. Electrochem. Sci. 2008;3:1-28.
6. Hurley BL, McCreery RL. Raman spectroscopy of monolayers formed from chromate corrosion inhibitor on copper surfaces. J. Electrochem. Soc. 2003;150: B367-B373.
7. Armour AW, Robitaille DR. Corrosion inhibition by sodium molybdate. J. Chem. Technol. Biotechnol. 1979;10:619-628.
8. Gece G. Drugs: A review of promising novel corrosion inhibitors. Corros. Sci. 2011;53:3873–3898.
9. Zhang DQ, Cai QR, He XM, Gao LX, Zhou GD. Inhibition effect of some amino acids on copper corrosion in HCl solution. Mater. Chem. Phys. 2008;112:353–358.
10. Kaya S, Tüzün B, Kaya C, Obot BI. Determination of corrosion inhibition effects of amino acids: Quantum chemical and molecular dynamic simulation study. J. Taiwan. Inst. Chem. Eng. 2015;58:528–535.
11. Sudheer MA Quraishi. Electrochemical and theoretical investigation of triazole derivatives on corrosion inhibition behaviour of copper in hydrochloric acid medium. Corros. Sci. 2013;70:161–169.
12. Bowmaker GA, Pakawatchai C, Skelton BW, Thanyasirikul Y, White AH. Structural and spectroscopic studies of $[M((x)tu)_4]^+$ Systems (M = Cu, Ag; (x)tu = (substituted) Thiourea). Z. Anorg. Chem. 2008;14:2583–2588.
13. Chuaysong R, Chooto P, Pakawatchai C. Electrochemical properties of copper (I) halides and substituted thiourea complexes. Science Asia. 2008;34:440-442.
14. Taylor IF, Weininger MS, Amma EL. Preparation, crystal structure, and bonding in the dimers of tris (thiourea) coppers (I) tetrafluoroborate and tris(s-dimethyl-thiourea) copper (I) tetrafluoroborate. Inorg. Chem. 1974;13:2835–2842.
15. Souza FSD, Giacomelli C, Gonçalves RS, Spinelli A. Adsorption behavior of caffeine as a green corrosion inhibitor for copper. Mater. Sci. Eng. 2012;32:2436–2444.
16. Stoyanova Slavcheva E. Effect of the molecular structure of some quinones on their corrosion inhibiting action. Mater. Corr. 2011;62:872-877.
17. Amin MA, Khaled KF. Copper corrosion inhibition in O_2-saturated H_2SO_4 solutions. Corros.Sci. 2010;52:1194–1204.
18. Eldesoky AM. Hassan HM, Foufa AS. Studies on the corrosion inhibition of copper in nitric acid solution using some pharmaceutical compounds. Int. J. Electrochem. Sci. 2013;8:10376-10395.
19. Fouda AS Wahed. Corrosion inhibition of copper in HNO_3 solution using thiophene and its derivatives. Arab. J. Chem. 2016; 9:S91-S99.
20. Khaled KF, Hackerman N. Ortho-substituted anilines to inhibit copper corrosion in aerated 0.5 M hydrochloric acid. Electrochim. Acta. 2004;49:485-495.
21. Sherif El-Sayed M, Erasmus RM, Comins JD. Corrosion of copper in aerated synthetic sea water solutions and its inhibition by 3-amino-1,2,4-triazole. J. Colloid Interface Sci. 2007;309:470-477.
22. Wedian F, Al-Qudah MA, Al-Mazaideh GM. Corrosion inhibition of copper by *Capparis spinose* L. extract in strong acidic medium: Experimental and density functional theory. Int. J. Electrochem. Sci. 2017;12:4664-4676.
23. Hegazy MA, Nazeer AA, Shalabi K. Electrochemical studies on the inhibition behavior of copper corrosion in pickling

acid using quaternary ammonium salts. J. Mol. Liq. 2015;209:419-427.

24. Yadav S, Choudhary G, Sharma A. Green approach to corrosion inhibition of aluminium and copper by *Ziziphus mauritiana* fruit extract in hydrochloric acid solution. Inter. J. Chem Tech. Res. 2013; 5:1815-1823.

25. Kalsi PS. Spectroscopy of organic compounds, sixth ed., New Age Int. (Pvt.) Ltd. Publishers, New Delhi; 2008.

26. Liu P, Fang X, Tang Y, Sun C, Yao C. Electrochemical and quantum chemical studies of 5-substituted tetrazoles as corrosion inhibitors for copper in aerated 0.5 M H_2SO_4 solution. Mater. Sci. Appl. 2011;2:1268-1278.

27. Raafat MI, Mohamed KA, Faten MA. Quantum chemical studies on the inhibition of corrosion of copper surface by substituted uracils. Appl. Surf. Sci. 2008;255:2433-2441.

Peer-review history:
The peer review history for this paper can be accessed here:
http://sciencedomain.org/review-history/20304